THE JOURNAL OF BIOLOGICAL CHEMISTRY VOL. 281, NO. 47, pp. 36110–36118, NOVEMBER 24, 2006

DNA Unwinding by *Escherichia coli* DNA Helicase I (TraI) Provides Evidence for a Processive Monomeric Molecular Motor*[S]

Received for publication, May 9, 2006, and in revised form, August 31, 2006 Published, JBC Papers in Press, September 19, 2006, DOI 10.1074/jbc.M604412200

Bartek Sikora[‡1], **Robert L. Eoff**[‡1], **Steven W. Matson**[§], **and Kevin D. Raney**[‡2]

From the [‡]*Department of Biochemistry and Molecular Biology, University of Arkansas for Medical Sciences, Little Rock, Arkansas 72205 and the* [§]*Department of Biology, Curriculum in Genetics & Molecular Biology, Program in Molecular & Cellular Biophysics, University of North Carolina, Chapel Hill, North Carolina 27599-3280*

The F plasmid TraI protein (DNA helicase I) plays an essential role in conjugative DNA transfer as both a transesterase and a helicase. Previous work has shown that the 192-kDa TraI protein is a highly processive helicase, catalytically separating >850 bp under steady-state conditions. In this report, we examine the kinetic mechanism describing DNA unwinding of TraI. The kinetic step size of TraI was measured under both single turnover and pre-steady-state conditions. The resulting kinetic step-size estimate was ~6–8 bp step^{-1}. TraI can separate double-stranded DNA at a rate of ~1100 bp s^{-1}, similar to the measured unwinding rate of the RecBCD helicase, and appears to dissociate very slowly from the 3′ terminus following translocation and strand-separation events. Analyses of pre-steady-state burst amplitudes indicate that TraI can function as a monomer, similar to the bacteriophage T4 helicase, Dda. However, unlike Dda, TraI is a highly processive monomeric helicase, making it unique among the DNA helicases characterized thus far.

The nature of cellular processes involves manipulation of nucleic acids for diverse metabolic events such as replication, recombination, repair, transcription, translation, and splicing of transcripts (1). Helicases are a ubiquitous class of enzymes that couple the chemical energy associated with NTP hydrolysis with the mechanical manipulation of nucleic acids (2). Traditionally, helicases are described as having the ability to catalyze the thermodynamically unfavorable separation of double strand nucleic acid to form transient single strand nucleic acid intermediates (3). However, it has become clear that many helicase-like proteins perform additional and/or disparate functions beyond simple unwinding of double strand nucleic acid (4). These additional processes include removal of protein blocks from the path of macromolecular machinery through generation of a directional force, transport of nucleic acid from one point in the cell to another, and packaging of viral nucleic acid (5–8).

DNA helicase I (TraI) is a bifunctional protein encoded by the *Escherichia coli* F-plasmid (9) that contains three functional domains essential for transfer of bacterial genes during conjugation (10–12). Catalytically, TraI is a 192-kDa ssDNA[3] dependent NTPase that possesses both helicase and transesterase activities (11). Previous work has shown that TraI translocates with a 5′ to 3′ directional bias and requires at least 20 nt of ssDNA for unwinding of dsDNA *in vitro* (13, 14). Furthermore, TraI can separate at least 850 bp of dsDNA under steady-state conditions (14). Early reports suggested that the enzyme functions in a multimeric state, as evidenced by formation of aggregates at low ionic strength and low ATPase activity at KCl concentrations >150 mM (15–17). A later study suggested the possibility that TraI could function as a monomer (14). An analysis of the kinetic mechanism describing TraI helicase activity has not been performed to date. Rapid-quench flow experiments were performed under a variety of conditions to address the transient state kinetics associated with TraI-catalyzed unwinding of dsDNA. Specifically, the kinetic step size of TraI was measured using experimental approaches and numerical techniques described previously (18–20). Pre-steady-state experiments were also performed to address whether TraI kinetic parameters change under conditions favoring monomeric forms of the enzyme. The results reported herein provide evidence that TraI can function as a processive monomeric helicase.

EXPERIMENTAL PROCEDURES

Materials—ATP (disodium salt) and Sephadex (G-25) were obtained from Sigma. HEPES, Na_4EDTA, β-mercaptoethanol, bovine serum albumin, $Mg(OAc)_2$, KOAc, SDS, xylene cyanol, bromphenol blue, NaCl, glycerol, and KOH were obtained from Fisher. T4 polynucleotide kinase was purchased from New England Biolabs. [γ-^{32}P]ATP was purchased from New England Nuclear. DNA oligonucleotides (Integrated DNA Technologies, Coralville, IA) were purified by preparative PAGE and stored in 10 mM HEPES (pH 7.5) and 1 mM EDTA. All oligonucleotides were resuspended in 10 mM HEPES/1 mM EDTA, pH

* This work was supported by National Institutes of Health (NIH) Grant R01 GM059400 and the Arkansas Biosciences Institute (to K. D. R.) and by NIH Grant R01 GM61020 (to S. W. M.). The costs of publication of this article were defrayed in part by the payment of page charges. This article must therefore be hereby marked "*advertisement*" in accordance with 18 U.S.C. Section 1734 solely to indicate this fact.

[S] The on-line version of this article (available at http://www.jbc.org) contains supplemental Fig. S1 and Table S1.

[1] Both authors contributed equally to this work.

[2] To whom correspondence should be addressed: Dept. of Biochemistry & Molecular Biology, University of Arkansas for Medical Sciences, Slot 516, 4301 W. Markham St., Little Rock, AR 72205. Tel.: 501-686-5244; Fax: 501-686-8169; E-mail: raneykevind@uams.edu.

[3] The abbreviations used are: ssDNA, single strand DNA; dsDNA, double strand DNA; nt, nucleotide(s); MOPS, 4-morpholinepropanesulfonic acid; NLLS, non-linear least squares.

7.5. Recombinant TraI was purified as described (11, 14) and quantified by UV absorbance at 280 nm using an extinction coefficient of 129,795 M^{-1} cm^{-1}.

Helicase Substrates—The sequences for the DNA substrates used in this study are listed in supplemental Table S1. The loading strand of each substrate was radiolabeled. Purified oligonucleotides were 5′-radiolabeled with T4 polynucleotide kinase at 37 °C for 1 h. The kinase was inactivated by heating to 70 °C for 10 min, and unincorporated [γ-^{32}P]ATP was removed by passing the reaction mixture over two Sephadex G-25 columns. Helicase substrates were prepared by adding 1.5 equivalents of the complementary oligonucleotide to the 5′-radiolabeled oligonucleotide, followed by heating to 95 °C for 10 min, and then slow cooling to room temperature.

Rapid Quench-flow Helicase Unwinding Experiments—Unwinding assays were performed with a rapid chemical quench-flow instrument (Kintek, Austin, TX) maintained at 25 °C (unless otherwise stated) with a circulating water bath. All concentrations listed are after mixing, unless otherwise stated. The helicase reaction buffer consisted of 25 mM MOPS, pH 7.0, 0.1 mg/ml bovine serum albumin, and 10 mM NaCl. TraI was stored and when necessary diluted in 20 mM Tris-HCl, pH 7.5, 0.1 mM Na_4EDTA, pH 8.0, 200 mM NaCl, and 50% glycerol prior to performing the unwinding assays. For pre-steady-state experiments TraI (final concentration of 40 nM) was incubated on ice for 2–5 min with 100 nM radiolabeled DNA substrate and reaction buffer. For the excess enzyme experiments, TraI (final concentration of 200 nM or 100 nM) was incubated for 2–5 min with 2 nM radiolabeled DNA substrate and reaction buffer. When single-turnover conditions were required 10 μM poly(dT) was included to prevent TraI from re-binding to the radiolabeled substrate following the first catalytic turnover. Unless otherwise stated, the reaction was initiated by adding 5 mM ATP, 10 mM $Mg(OAc)_2$, and 30-fold excess re-annealing trap. The sequence of the re-annealing trap is complementary to the displaced strand of the substrate so that re-annealing of the displaced strand to the radiolabeled loading strand was prevented following TraI-catalyzed separation. The reaction mixture was rapidly mixed with 200 mM EDTA/0.7% SDS to quench the reaction following the allotted timeframe. 25 μl of the quenched solution was then added to 5 μl of non-denaturing gel loading buffer (0.1% bromphenol blue, 0.1% xylene cyanol in 6% glycerol). Finally, the dsDNA substrate was separated from ssDNA product on a 20% native polyacrylamide gel. Supplemental Fig. S1 shows two representative gels. Radiolabeled substrate and product were visualized by using a Molecular Dynamics PhosphorImager and ImageQuaNT software. The quantity of radioactivity was used to determine the ratio of double-stranded oligonucleotide substrate to single-stranded oligonucleotide product as a function of time.

Non-linear Least Squares Analysis of Unwinding Data—TraI-catalyzed unwinding of varying lengths of dsDNA was analyzed using the *n*-step sequential mechanism shown in the scheme given in Fig. 3. Such analyses have been performed previously, and the numerical techniques have been described in rigorous detail (20). Data fitting was performed using the program Scientist (Micromath, St. Louis, MO). Equation 1 represents the analytic expression describing the time-dependent formation of ssDNA product, $f_{ss}(t)$, for the reaction scheme (see Fig. 3), as has been defined previously (18–20),

$$f_{ss}(t) = A_T\left[\left(1 - \sum_{r=1}^{n}\frac{((k_u)t)^{r-1}}{(r-1)!}e^{-(k_u)t}\right) - e^{-k_{NP}t}(1-x) \times \left(\frac{k_u}{k_u + k_{NP}}\right)^n\left(1 - \sum_{r=1}^{n}\frac{((k_u - k_{NP})t)^{r-1}}{(r-1)!} \times e^{-(k_u - k_{NP})t}\right)\right] \quad \text{(Eq. 1)}$$

where x represents the fraction of productively bound complexes given by Equation 2, and A_T is the total unwinding amplitude.

$$x = \frac{ES_{L_T}}{ES_{L_T} + ES_{NP}} \quad \text{(Eq. 2)}$$

The method of Laplace transforms has been used previously to solve the system of differential equations for the reaction scheme (see Fig. 3) (19, 20). The resulting expression $F_{ss}(s)$ is the Laplace transform of Equation 1, describing the minimal reaction scheme for unwinding by a helicase that does not dissociate readily from the DNA substrate lengths used for *in vitro* unwinding assays,

$$F_{ss}(s) = \frac{k_u^n(k_{NP} + sx)}{s(k_{NP} + s)(k_u + s)^n} \quad \text{(Eq. 3)}$$

where s is the Laplace variable of the fraction of ssDNA product formed over time, $f_{ss}(t)$ (Equation 1). The inverse Laplace transform, $\mathcal{L}^{-1}$, can then be obtained using the numerical integration capabilities of Scientist to obtain $f_{ss}(t)$ as shown in Equation 4.

$$f_{ss}(t) = \mathcal{L}^{-1}(F_{ss}(s)) = \left(\frac{k_u^n(k_{NP} + sx)}{s(k_{NP} + s)(k_u + s)^n}\right) \quad \text{(Eq. 4)}$$

The reaction scheme (see Fig. 3) assumes that each step in the series along the unwinding pathway is identical. The kinetic step size (m) is then defined with Equation 5,

$$m = \frac{L_T - L_0}{n} \quad \text{(Eq. 5)}$$

where L_T equals the total length of dsDNA in bp, and L_0 equals the minimal length of dsDNA that is stable in the presence of an active helicase. By replacing n (in Equation 4) with Equation 5 and performing NLLS analysis of the subsequent expression, an estimate of m can be obtained.

RESULTS

Effect of ssDNA Overhangs and Fork Substrates on TraI-catalyzed Unwinding of dsDNA—Previously, TraI has been shown to require an ssDNA region of >20 nt to initiate unwinding under conditions allowing multiple enzymatic turnovers (13). Rapid-quench flow experiments were performed under excess-enzyme conditions with substrates containing a 5′-overhang of varying length or a fork substrate (Fig. 1). Results for TraI-catalyzed separation of fork substrate, 30 nt:30 bp, 45 nt:30 bp and 60 nt:30 bp are plotted in Fig. 1*B*. The amount of ssDNA

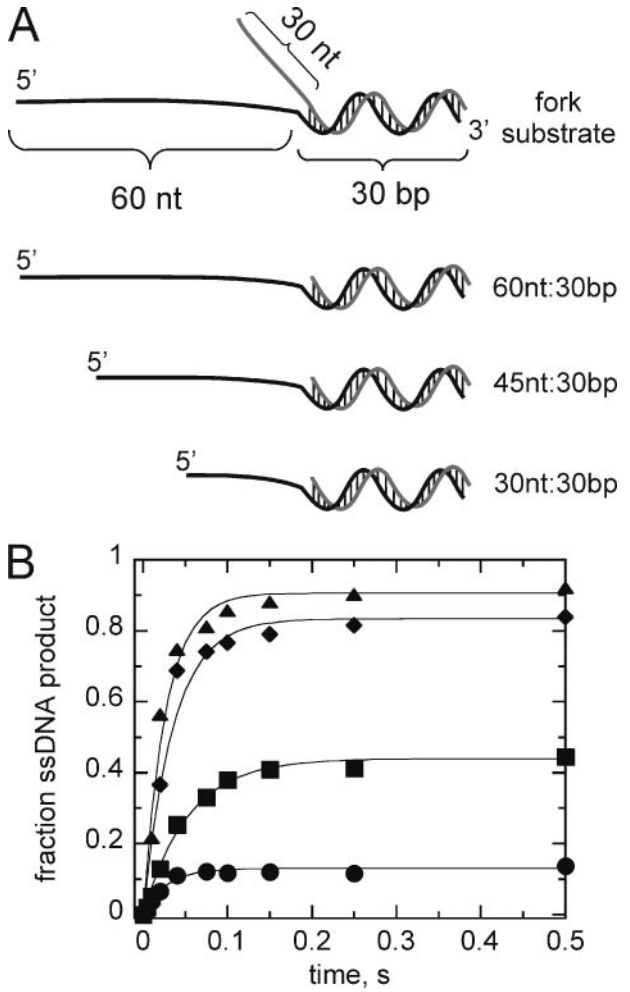

FIGURE 1. **Optimization of the substrate for DNA unwinding by TraI.** *A*, DNA substrates are shown with the 5′- and 3′-overhangs indicated. The substrates are named according to the length of the ssDNA overhang and the length of the duplex. The 60nt:30bp substrate contains 60 nt of ssDNA and 30 bp. *B*, results for DNA unwinding of substrates (2 nM) by TraI (200 nM) 30 nt:30 bp (●),45 nt:30 bp (■), 60 nt:30 bp (▲), and the fork substrate (◆). Data were fit to a single exponential (Equation 1) using the program KaleidaGraph™: $y = A_T[1 - \exp(-k_{obs}t)]$. The resulting kinetic parameters were as follows: ●, 30 nt:30 bp, $k_{obs} = 36 \pm 6\ s^{-1}$, $A = 0.26 \pm 0.01$ nM; ■, 45 nt:30 bp, $k_{obs} = 19 \pm 1\ s^{-1}$, $A = 0.88 \pm 0.02$; ▲, 60 nt:30 bp, $k_{obs} = 32 \pm 4\ s^{-1}$, $A = 1.81 \pm 0.06$ nM; ◆, fork substrate, $k_{obs} = 28 \pm 5\ s^{-1}$, $A = 1.67 \pm 0.08$ nM.

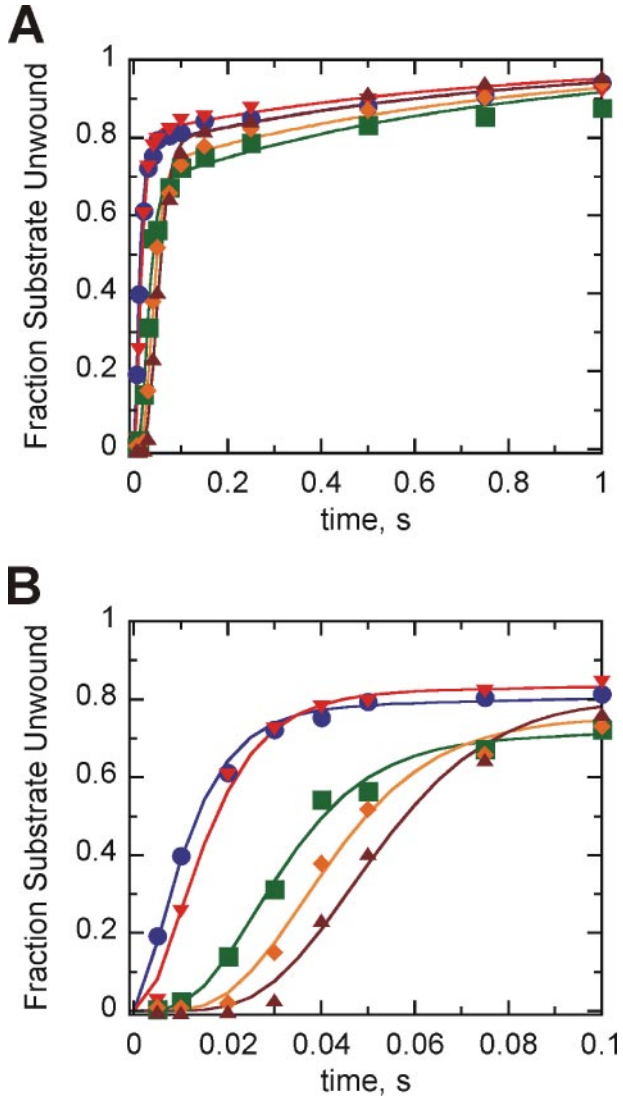

FIGURE 2. **TraI-catalyzed unwinding of varying lengths of dsDNA performed under excess-enzyme and single-turnover conditions.** *A*, results for 100 nM TraI-catalyzed unwinding of 2 nM 60 nt:15 bp (*blue* ●), 60 nt:22 bp (*red* ▼), 60 nt:30 bp (*green* ■), 60 nt:45 bp (*orange* ◆), and 60 nt:60 bp (*brown* ▲) shown to 1 s. The data were fit to Equation 4 using the program Scientist. The kinetic parameters are listed in Table 1. *B*, results from *panel A* shown to 0.1 s.

product increases as the ssDNA overhang length is increased. The presence of both a 5′- and 3′-overhang (fork substrate) did not enhance the rate of unwinding, indicating that a fork substrate is not required for TraI.

TraI-catalyzed Unwinding of Varying Lengths of dsDNA—The optimal ssDNA overhang contained 60 nt. The effect of varying duplex length was investigated by designing several substrates that contained a 60-nt overhang and 15, 22, 30, or 45 bp of duplex DNA. Single-turnover rapid-quench flow experiments were then performed under excess-enzyme conditions, and the results are shown in Fig. 2. Simultaneous NLLS analysis of the unwinding data for all five substrates resulted in the kinetic parameters listed in Table 1. All of the substrates are unwound to a similar extent, regardless of the length of the duplex, indicating that TraI does not dissociate from the substrate under these conditions. The progress curve for each substrate contains a slower phase, which accounts for the final

TABLE 1
Global kinetic parameters determined from NLLS

Conditions	k_u	k_{NP}	Average m	Average mk_U
	s^{-1}		*bp step*$^{-1}$	*bp* s^{-1}
Excess TraI[a]	137 ± 11	1.4 ± 0.1	8.2 ± 1.1	1120 ± 160
Excess DNA[b]	175 ± 30	0.9 ± 0.1	6.2 ± 0.5	1085 ± 90
Local kinetic parameters for different lengths of dsDNA				
dsDNA length	***m* excess TraI**		***m* excess DNA**	
bp	*bp step*$^{-1}$			
15	8.9 ± 0.6		6.7 ± 1.0	
22	9.6 ± 0.7		5.6 ± 0.9	
30	6.6 ± 0.5		5.8 ± 1.0	
45	7.6 ± 0.6		6.2 ± 1.0	
60	8.2 ± 0.6		6.7 ± 1.0	

[a] Kinetic parameters obtained from fitting data in Fig. 2 to Equation 4 based on the reaction scheme (Fig. 3).
[b] Kinetic parameters obtained from fitting data in Fig. 6 to Equation 4 based on the reaction scheme (Fig. 3).

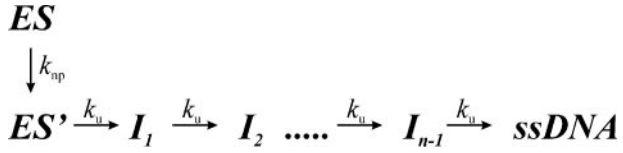

FIGURE 3. **Reaction scheme describing a series of *n*-sequential steps of helicase-catalyzed translocation and strand separation.** Each identical step in the reaction pathway is defined by a forward rate-constant, k_u. An additional step, k_{np}, occurs at the outset of the unwinding reaction, which has been correlated with an isomerization step that precedes DNA unwinding.

fraction of ssDNA product. This slower phase appears despite the inclusion of a protein trap in the reaction mixture. Therefore, the slower phase is likely due to the formation of a small quantity of non-productive enzyme-substrate complex that slowly isomerizes to form productive enzyme-substrate complex as has been described for other helicases such as Rep (21) and UvrD (18). The longer substrates exhibit a lag phase in the early portion of the unwinding progress curve (Fig. 2*B*). The lag phase increases with increasing duplex length, consistent with a stepping mechanism.

The reaction scheme (Fig. 3) shows a stepwise mechanism that can account for the lag phase observed in DNA unwinding. The scheme includes a step for slow isomerization of a non-productive, enzyme-substrate complex. Because all of the amplitudes are similar and are close to complete unwinding, these relatively short DNA substrates cannot be utilized to discern dissociation constants of the enzyme from the DNA substrate. Hence, dissociation is not included in the kinetic mechanism in the reaction scheme. Based on previous work from Lucius *et al.* (19, 20), we applied Equation 4 to globally fit data in Fig. 2 to obtain rate constants for unwinding as well as the number of base pairs unwound per kinetic step (or step size). The resulting kinetic parameters are shown in Table 1. TraI unwound the DNA very rapidly with an average rate constant of 137 s^{-1} per kinetic step and an average kinetic step size of 8.2 ± 1.1 bp. These values correspond to a rate of 1120 ± 160 bp s^{-1} for DNA unwinding making TraI one of the fastest helicases studied to date. For comparison, RecBCD has been shown to unwind dsDNA at a rate of ~790 bp s^{-1} at 25 °C (19) when measured using oligonucleotide substrates and ~970 bp s^{-1} when measured by direct observation of single RecBCD molecules (22).

DNA Unwinding under Steady-state Conditions—Previous work with the NS3 helicase domain indicated that the ssDNA overhang could bind multiple molecules of enzyme and that more molecules bound to the same substrate led to greater activity (23). Similar behavior was observed with Dda helicase, whereby multiple molecules of enzyme bound to the same strand of DNA produced greater enzymatic activity for DNA unwinding (24) and for displacement of streptavidin from biotinylated DNA (6). TraI required a relatively long ssDNA overhang (60 nt) for optimal activity, indicating that similar behavior might be exhibited by this enzyme. Experiments were conducted under steady-state conditions to determine whether multiple TraI molecules could bind to the 60-nt overhang and perhaps exhibit cooperativity for DNA unwinding. Steady-state conditions were examined in which the concentration of DNA substrate was in excess of TraI (Fig. 4). The resulting rates for

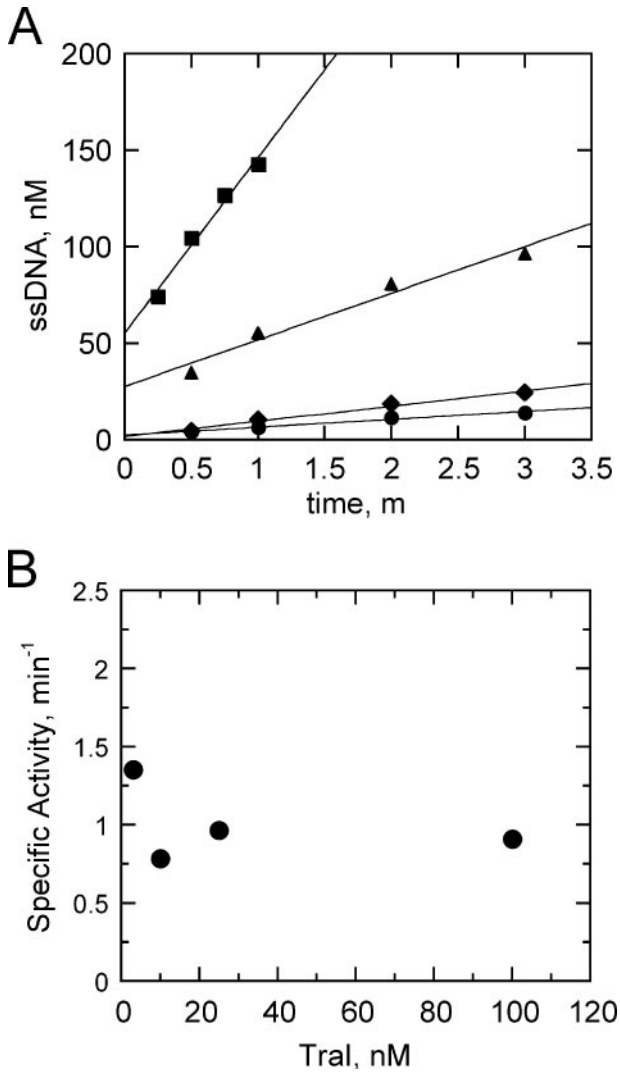

FIGURE 4. **Steady-state DNA unwinding at varying concentrations of TraI.** *A*, the 60 nt:30 bp substrate (250 nM) was incubated with 3 nM (●), 10 nM (♦), 25 nM (▲), or 100 nM (■) TraI. ssDNA product is plotted, and data were fit to a linear function. *B*, the specific activity determined from rates measured in *panel A* is plotted as a function of TraI concentration.

unwinding were plotted as a function of TraI concentration, resulting in no apparent increase in the specific activity of the enzyme (Fig. 4*B*). An additional feature of the steady state results was the positive intercept of the unwinding plots observed at higher concentrations of TraI (filled squares and filled triangles in Fig. 4*A*). The positive intercept suggested that TraI might exhibit a "burst amplitude" under pre-steady state conditions as was observed previously with Dda helicase (25).

Pre-steady-state Unwinding of dsDNA by TraI—Varying concentrations of TraI were incubated with an excess of the 60 nt:22 bp substrate, and the unwinding reaction was initiated by rapid mixing with ATP. The resulting data clearly exhibit a burst amplitude for ssDNA product formation (Fig. 5). The initial burst phase is complete at ~30 ms and is followed by a slower phase in which ssDNA product continues to form. This slow phase is reminiscent of the slow phase observed in the single turnover experiments, which was attributed to a slow isomerization of non-productively bound enzyme (Fig. 2). By definition, the pre-steady state experiments are con-

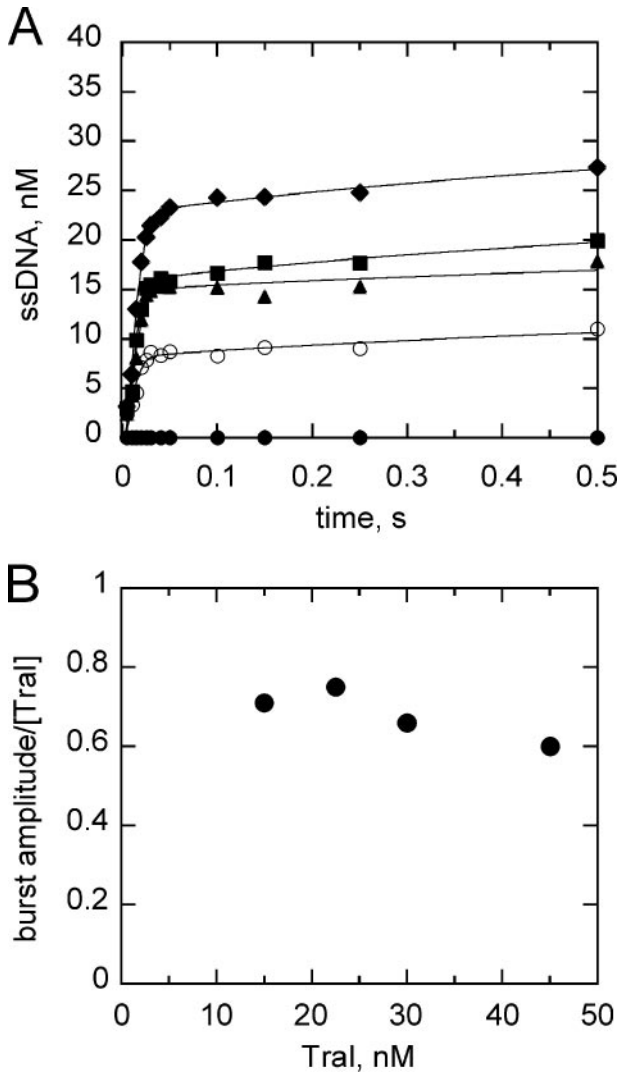

FIGURE 5. **DNA unwinding by TraI under pre-steady-state conditions.** *A*, varying concentration of TraI was incubated with 100 nM DNA substrate (60 nt:22 bp) followed by initiation of the reaction by mixing with ATP. The ssDNA product formed over the first 0.5 s is plotted TraI concentration of 15 nM (○), 22.5 nM (▲), 30 nM (■), and 45 nM (♦). Data were fit to the reaction scheme (Fig. 3) using the program Scientist and limiting the number of sequential steps for unwinding to three. TraI (40 nM) was mixed with 100 nM DNA (60 nt:22 bp) along with ATP and Mg^{+2} (●). *B*, the concentration of ssDNA formed after 0.5 s of reaction time (burst amplitude) divided by the concentration of TraI is plotted *versus* the TraI concentration.

ducted in the absence of a protein trap so that a steady-state phase can ensue after the burst phase. To determine whether the slow phase exhibited under pre-steady-state conditions represents a slow isomerization or a steady state, an experiment was conducted in which TraI was rapidly mixed with substrate and ATP. The experiment effectively measures whether free TraI in solution has time to bind to substrate and unwind the DNA during the first 0.5 s of the reaction. As seen in Fig. 5*A*, no product was observed under these conditions (*filled circles*). Therefore, under these conditions, TraI that is free in solution does not rapidly associate with and unwind the DNA substrate during the initial 0.5 s of the reaction. Therefore, the slow phase observed in pre-steady-state experiments was due to a slow isomerization, as was observed under single-turnover conditions. The data in Fig.

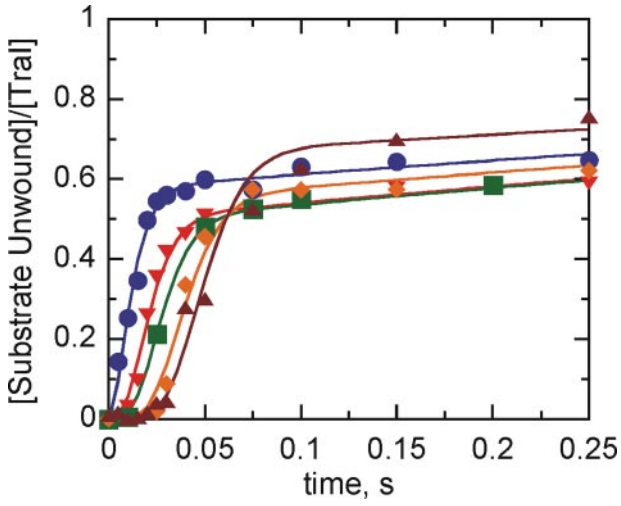

FIGURE 6. **Pre-steady-state analysis of TraI-catalyzed unwinding of varying lengths of dsDNA.** Results are shown for 40 nM TraI-catalyzed unwinding of 100 nM 60 nt:15 bp (*blue* ●), 60 nt:22 bp (*red* ▼), 60 nt:30 bp (*green* ■), 60 nt:45 bp (*orange* ♦), and 60 nt:60 bp (*brown* ▲). The data were fit to Equation 4 using the program Scientist. The kinetic parameters are listed in Table 1.

5 were fit to a three-step mechanism, including a slow isomerization step similar to that in the reaction scheme (Fig. 3).

The burst amplitude of ssDNA during the first 0.5 s corresponds to the concentration of TraI that is capable of forming ssDNA. The amplitude was divided by the TraI concentration and plotted *versus* TraI concentration in Fig. 5*B*. The resulting amplitudes range from 0.6 to 0.75, which is consistent with a monomeric form of TraI because the amplitudes are >0.5, or 50% of the available enzyme.

Kinetic Step Size Determined under Pre-steady-state Conditions—Pre-steady-state conditions clearly favor a monomeric form of TraI. The kinetics of DNA unwinding were determined under these conditions to compare them to those obtained under single turnover, excess enzyme conditions. Unwinding was measured with 40 nM TraI and 100 nM substrate for the five DNA substrates (Fig. 6). The amount of time required for product to form increases as a function of dsDNA length, consistent with a stepping mechanism, and the time courses resemble the data from single-turnover experiments. Simultaneous, NLLS analysis of the unwinding data for all five substrates resulted in the kinetic parameters listed in Table 1.

The amplitudes for all five substrates are very similar, which is consistent with TraI being a highly processive helicase. In contrast, Dda helicase from bacteriophage T4 can clearly function as a monomer (25), but it does so in a non-processive manner. Dda exhibits >85% burst amplitude for unwinding short 12- to 16-bp substrates (25), but the burst amplitude for Dda-catalyzed unwinding of substrates decreases for every base pair added to the dsDNA length (26). Monomeric TraI exhibits a ~70% burst amplitude when unwinding 60 bp, making TraI one of the first documented cases of a highly processive monomeric helicase.

DISCUSSION

The kinetic mechanism describing TraI-catalyzed unwinding of dsDNA was investigated using transient-state kinetic

approaches. Increasing the ssDNA overhang increases the amplitude of TraI-catalyzed unwinding (Fig. 1), consistent with previous steady-state analysis of TraI activity (13). The lack of complete unwinding of the shorter substrates might be due to poor binding of TraI. For example, association of TraI with the short substrates appears to lead to substantial amounts of non-productively bound substrate. Rapid dissociation and re-association of substrate with TraI may not occur during the short time frame for this experiment (0.5 s). Further experiments were performed under single-turnover conditions with respect to the DNA substrate. Product formation occurred in a bi-phasic manner, even in the presence of a protein trap (Fig. 2). TraI-catalyzed unwinding of dsDNA proceeded at a very rapid rate ($\sim$1100 bp s^{-1}), as determined from NLLS fitting of the data in Fig. 2 to Equation 4, which is derived from the reaction scheme (Fig. 3). An interesting feature of both the pre-steady-state and excess enzyme experiments is the similar product amplitude obtained for all lengths of dsDNA tested. TraI readily unwound substrates up to 60 bp in length, indicating that this helicase is highly processive. Attempts to determine the dissociation constant by fitting the data in Fig. 2 to schemes that allow for enzyme dissociation led to dissociation rate constants that were close to zero with very high errors (not shown). The relatively short duplexes used in this study are insufficient to provide an accurate measure of TraI processivity.

The long ssDNA overhang required for optimal DNA unwinding activity was reminiscent of recent studies with other helicases such as NS3h (23) and Dda (24). NS3h and Dda are non-processive helicases that dissociate prior to completion of unwinding leading to inefficient unwinding of longer DNA substrates. Multiple molecules of NS3h have been proposed to increase the quantity of DNA unwinding through "functional cooperativity" (23). In this model, trailing molecules of helicase complete the unwinding process after leading molecules dissociate from the substrate.

We examined TraI-catalyzed DNA unwinding under steady-state conditions to determine whether cooperativity could be observed. However, the specific activity for DNA unwinding did not increase with increasing concentration of TraI (Fig. 4). More precise examination of DNA unwinding by TraI under pre-steady-state conditions was performed to observe whether TraI could function as a monomeric helicase (Fig. 5). By placing DNA substrate in excess of TraI, the distribution of TraI species bound to any single DNA substrate favors the monomeric state. A burst in product formation that is $>$50% of the total enzyme concentration in the reaction is indicative of a monomeric enzyme (25). Indeed, TraI produced a burst amplitude that was $>$50% (Fig. 5), even when the DNA duplex length was increased to 60 bp (Fig. 6). These results indicate that TraI can function as a helicase in the monomeric state.

Relating the kinetic step size to a physical step is an important goal toward understanding helicase mechanisms. Structural studies of PcrA helicase have been interpreted in terms of a 1-bp step size (27). Subsequent kinetic studies of PcrA translocation on ssDNA also provided a kinetic step size of 1 bp, correlating with the structural studies (28). By varying the length of dsDNA, the TraI kinetic step size was measured to be 8.2 $\pm$ 1.1 bp per step under excess-enzyme conditions (Table 1). A similar step size of 6.2 $\pm$ 0.5 bp was determined under pre-steady-state conditions. A physical description of the kinetic step size for TraI remains to be determined. For comparison, the kinetic step size determined for other helicases range from 3.9 bp for RecBCD (19), 4.5 bp for UvrD (18), and 1.4 bp for DnaB (29). RecBCD has two motors, each of which operates on one of the DNA strands (30, 31). UvrD functions as a dimer (32), and DnaB functions as a hexamer (33). The results reported thus far do not indicate any correlation between kinetic step size and the oligomeric state of the enzyme. The physical step size for a helicase may be directly related to the kinetic step size, as suggested in the case of DnaB (29). However, it is possible that multiple kinetic steps exist that make up the observed kinetic step. For example, a discrete step of $\sim$11 bp for NS3 was recently reported based on single molecule measurements (34). However, actual unwinding appeared to occur as smaller substeps of $\sim$3.6 bp. The oligomeric state of NS3 has not been clearly defined, but evidence for a monomeric form of the enzyme was presented in the single molecule experiments (34).

Galletto *et al.* (29) observed that plotting the number of kinetic steps as a function of duplex length provided evidence for spontaneous melting of the very end of the duplex. Recent work with the Dda helicase has shown that the final $\sim$8 bp of dsDNA melt spontaneously during unwinding (26). To accurately calculate the kinetic step size and unwinding rate associated with TraI catalysis, the number of base pairs catalytically separated by the enzyme must be known. An overestimate of both kinetic step size and unwinding rate will be obtained if spontaneous melting of the end of the substrate occurs but is not taken into account. The kinetic step size for TraI was plotted as a function of each duplex length under excess enzyme and pre-steady-state conditions (Fig. 7). Interestingly, when the data were fit to a linear function, the intercept was near zero under both conditions, indicating that little or no duplex DNA melted spontaneously during TraI-catalyzed unwinding. Therefore, we did not include spontaneous melting in the kinetic analysis of TraI-catalyzed DNA unwinding. This result might be explained by the fact that TraI is a 192-kDa helicase with multiple DNA binding domains (11). It is possible that TraI contains one or more domains that bind to the DNA substrate upstream and/or downstream of the helicase domain. For example, RecBCD helicase contains one domain that binds to the duplex region of the substrate (31). It is possible that such a domain might assist in preventing spontaneous melting of dsDNA by binding to the duplex, which would explain why spontaneous melting of the final base pairs is not observed.

In conclusion, transient-state kinetic analysis of TraI helicase activity indicates that TraI-catalyzed unwinding of dsDNA is both very rapid and highly processive. TraI can function as a monomeric helicase. The need for a very long ssDNA binding site suggests a role for DNA binding domains that are external to the helicase domain, which likely contributes to the high processivity of this enzyme. The lack of spontaneous melting of the final base pairs during DNA unwinding may further indicate that the DNA binding domains external to the helicase play some role in DNA unwinding.

Importantly, the properties described here and elsewhere (10, 13, 14) for TraI make this a unique DNA helicase. First, the

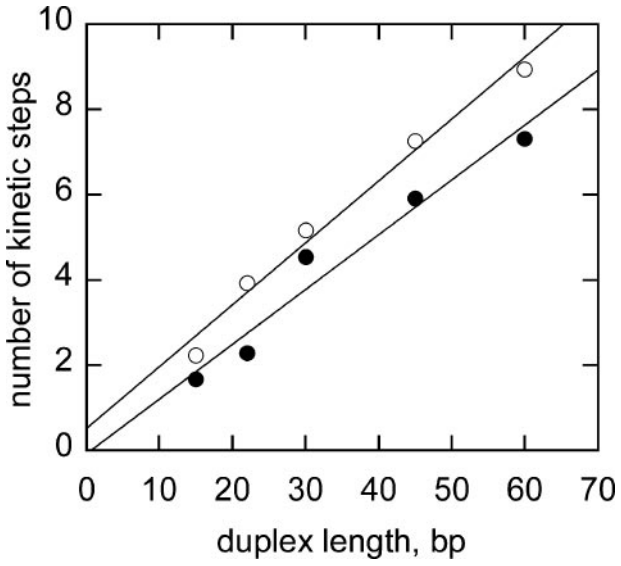

FIGURE 7. **Plot of the number of kinetic steps *versus* the length of ssDNA.** The kinetic steps obtained from NLLS fitting of data obtained under conditions of excess enzyme (●) or conditions of excess substrate (○). The data were fit to a linear function. The intercept for each fit was 0.52 and −0.07 under conditions of excess enzyme or excess substrate, respectively. The slope was 0.14 and 0.13 steps per base pair under conditions of excess enzyme or excess substrate, respectively.

unwinding rate reported here is faster than the unwinding rate reported for any helicase to date. TraI is known to unwind the 100-kbp F plasmid for transfer to recipient cells in a matter of a few minutes, consistent with this rate. In addition, when the F plasmid is integrated into the chromosome in Hfr strains, chromosomal DNA is transferred from the donor to the recipient. Classic mapping studies of the *E. coli* chromosome suggested the entire 4.6-Mbp chromosome could be transferred in ~100 min. If TraI-catalyzed unwinding of duplex DNA is the rate-limiting step in this process, then an unwinding rate of ~800 bp/s would be required to complete this event. This is very similar to the unwinding rate reported here. Second, TraI is a bifunctional protein that catalyzes a transesterase reaction in addition to the helicase reaction described here. The transesterase activity is required to initiate conjugative DNA transfer and results in covalent attachment of TraI to the 5′-end of the transferred DNA strand (10). A monomeric unwinding enzyme would be ideally positioned to complete the unwinding event required for DNA transfer. Finally, this is the first monomeric Superfamily I helicase that has been shown to catalyze a fast, processive unwinding reaction. Although the motor subunits of RecBCD are also Superfamily I helicases, these proteins do not appear to catalyze rapid, processive unwinding in the absence of the other components of the RecBCD complex (29). Thus, the biochemical characterization of TraI is consistent with the biological role this enzyme is believed to play in conjugative DNA transfer.

REFERENCES

1. Alberts, B. (1998) *Cell* **92,** 291–294
2. Delagoutte, E., and von Hippel, P. H. (2002) *Q. Rev. Biophys.* **35,** 431–478
3. Hall, M. C., and Matson, S. W. (1999) *Mol. Microbiol.* **35,** 867–877
4. von Hippel, P. H. (2004) *Nat. Struct. Mol. Biol.* **11,** 494–496
5. Bedinger, P., Hochstrasser, M., Jongeneel, C. V., and Alberts, B. M. (1983) *Cell* **34,** 115–123
6. Byrd, A. K., and Raney, K. D. (2004) *Nat. Struct. Mol. Biol.* **11,** 531–538
7. Byrd, D. R., Sampson, J. K., Ragonese, H. M., and Matson, S. W. (2002) *J. Biol. Chem.* **277,** 42645–42653
8. Lisal, J., and Tuma, R. (2005) *J. Biol. Chem.* **280,** 23157–23164
9. Geider, K., and Hoffmann-Berling, H. (1981) *Annu. Rev. Biochem.* **50,** 233–260
10. Matson, S. W., Sampson, J. K., and Byrd, D. R. (2001) *J. Biol. Chem.* **276,** 2372–2379
11. Matson, S. W., and Ragonese, H. (2005) *J. Bacteriol.* **187,** 697–706
12. Willetts, N., and McIntire, S. (1979) *Contrib. Microbiol. Immunol.* **6,** 137–145
13. Csitkovits, V. C., and Zechner, E. L. (2003) *J. Biol. Chem.* **278,** 48696–48703
14. Lahue, E. E., and Matson, S. W. (1988) *J. Biol. Chem.* **263,** 3208–3215
15. Abdel-Monem, M., Durwald, H., and Hoffmann-Berling, H. (1976) *Eur. J. Biochem.* **65,** 441–449
16. Abdel-Monem, M., and Hoffmann-Berling, H. (1976) *Eur. J. Biochem.* **65,** 431–440
17. Abdel-Monem, M., Lauppe, H. F., Kartenbeck, J., Durwald, H., and Hoffmann-Berling, H. (1977) *J. Mol. Biol.* **110,** 667–685
18. Ali, J. A., and Lohman, T. M. (1997) *Science* **275,** 377–380
19. Lucius, A. L., Vindigni, A., Gregorian, R., Ali, J. A., Taylor, A. F., Smith, G. R., and Lohman, T. M. (2002) *J. Mol. Biol.* **324,** 409–428
20. Lucius, A. L., Maluf, N. K., Fischer, C. J., and Lohman, T. M. (2003) *Biophys. J.* **85,** 2224–2239
21. Bjornson, K. P., Amaratunga, M., Moore, K. J., and Lohman, T. M. (1994) *Biochemistry* **33,** 14306–14316
22. Bianco, P. R., Brewer, L. R., Corzett, M., Balhorn, R., Yeh, Y., Kowalczykowski, S. C., and Baskin, R. J. (2001) *Nature* **409,** 374–378
23. Levin, M. K., Wang, Y. H., and Patel, S. S. (2004) *J. Biol. Chem.* **279,** 26005–26012
24. Byrd, A. K., and Raney, K. D. (2005) *Biochemistry* **44,** 12990–12997
25. Nanduri, B., Byrd, A. K., Eoff, R. L., Tackett, A. J., and Raney, K. D. (2002) *Proc. Natl. Acad. Sci. U. S. A.* **99,** 14722–14727
26. Eoff, R. L., and Raney, K. D. (2006) *Nat. Struct. Mol. Biol.* **13,** 242–249
27. Velankar, S. S., Soultanas, P., Dillingham, M. S., Subramanya, H. S., and Wigley, D. B. (1999) *Cell* **97,** 75–84
28. Dillingham, M. S., Wigley, D. B., and Webb, M. R. (2000) *Biochemistry* **39,** 205–212
29. Galletto, R., Jezewska, M. J., and Bujalowski, W. (2004) *J. Mol. Biol.* **343,** 83–99
30. Dillingham, M. S., Spies, M., and Kowalczykowski, S. C. (2003) *Nature* **423,** 893–897
31. Singleton, M. R., Dillingham, M. S., Gaudier, M., Kowalczykowski, S. C., and Wigley, D. B. (2004) *Nature* **432,** 187–193
32. Maluf, N. K., Fischer, C. J., and Lohman, T. M. (2003) *J. Mol. Biol.* **325,** 913–935
33. Bujalowski, W., Klonowska, M. M., and Jezewska, M. J. (1994) *J. Biol. Chem.* **269,** 31350–31358
34. Dumont, S., Cheng, W., Serebrov, V., Beran, R. K., Tinoco, I., Jr., Pyle, A. M., and Bustamante, C. (2006) *Nature* **439,** 105–108